

Substitution reactions on cyclometallated Pt(IV) complexes; a kinetic survey of the bond strength of Pt–S, N, and P-based ligands

Julio Esteban^a, Mercè Font-Bardia^b, Carlos Gallego^a, Gabriel González^a,
Manuel Martínez^{a,*}, Xavier Solans^b

^a *Department de Química Inorgànica, Universitat de Barcelona, Martí i Franquès 1-11, E-08028 Barcelona, Spain*

^b *Departament de Cristal·lografia, Mineralogia i Dipòsits Minerals, Universitat de Barcelona, Martí i Franquès s/n, E-08028 Barcelona, Spain*

Received 17 February 2003; accepted 22 February 2003

Abstract

The substitution reactions of a series of sulfur, nitrogen and phosphorus-based ligands (L) on Pt(IV) complexes having a chloride ligand, the cyclometallated imine ligand $CC_5Cl_4CHNCH_2C_6H_5$, and two methyl groups and the leaving ligand in a *mer*-geometrical arrangement, $[Pt(C^{\wedge}N)(CH_3)_2Cl(L)]$, have been studied as a function of temperature, solvent, and electronic and steric characteristics of the leaving ligands. Although in all cases a limiting dissociative mechanism has been found to apply, where the dissociation of the leaving ligand corresponds to the rate-determining step, the relative values of the different rate constants involved in the process, i.e. dissociation/association of the leaving/entering ligands and the effect of the solvent, change dramatically in the systems studied. The results agree with the previously determined mechanism operating on these substitution reactions, and serve as a very good measure of the strength of the Pt–L bond, which is influenced by both electronic and steric characteristics. The possible solvent-assisted hydrogen bonding of the leaving ligand with the rest of the molecule is made also evident in the relevant situations. The equilibrium constants detected for some of the systems indicate that, although Pt(IV) complexes are expected to be hard acids and prefer nitrogen to sulfur or phosphorus donors, this is not so. This result is in line with the softening of the nature of the Pt(IV) centres of complexes containing several Pt–C bonds.

© 2003 Published by Elsevier Science B.V.

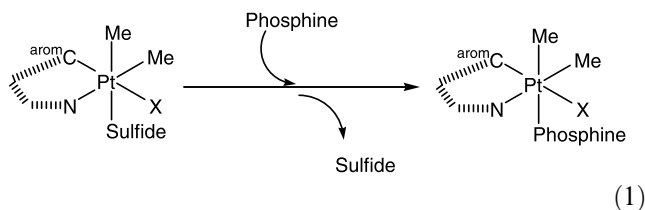
Keywords: Pt(IV) complexes; Solvent; Substitutions; Kinetics

1. Introduction

Although substitution processes taking place on inert t_{2g}^6 metal complexes are a clear candidate for mechanistic studies [1], only Co(III), Rh(III), and Fe(II) complexes have produced an important database [2]. Pt(IV) complexes, have been seldom used for this purpose in spite of the inherent importance of platinum chemistry in oxidative addition–reductive elimination reactions [3,4], hydrido complexes [5], and the Pt(IV)–Pt(II) reduction processes involved in the new generation of anticancer platinum pharmaceuticals [6–8]. In any of these processes the initial substitution reaction is

crucial, but poorly understood; redox assisted substitution has always prevented its proper study [9].

We have been involved lately in the mechanistic study of the substitution reactions on a series of cyclometallated complexes that allowed the clean presence of Pt(IV) centres (Eq. 1) [10–12].



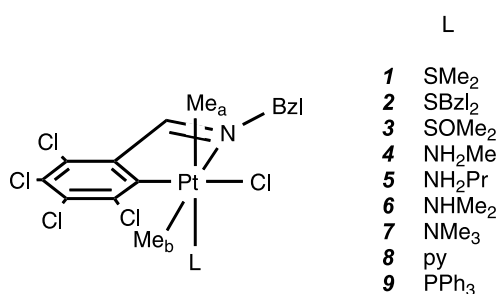
In most of the cases, a sulfide dissociation reaction to produce a pentacoordinated intermediate, that subsequently associates with the entering phosphine ligand has been proposed [10,13]; a direct associative process

* Corresponding author. Tel.: +34-934-021 273; fax: +34-934-907 725.

E-mail address: manel.martinez@qi.ub.es (M. Martínez).

for systems having both important hydrogen bonding possibilities, and electron withdrawing ligands, has also been seen to operate [11]. Following on this line, we decided to study the substitution reactions of a series of S, N, and P-based leaving ligands, the goal being the study of possible enhanced hydrogen bonding in the transition state [14], and the effect produced on the introduction of harder ligands, with relatively small cone angles and/or high basicity, as leaving ligands [15–17].

We present in this paper the study of the substitution processes of the complexes indicated in Scheme 1 with entering ligands (E) MeNH₂, PrNH₂, Me₂NH, Me₃N, py and PPh₃, in acetone and toluene solutions at different temperatures and in various solvents to produce the corresponding substituted compounds.



Scheme 1.

For this purpose all starting complexes involved, not previously characterized (3, 4, 5, 6, 7, 8), have also been prepared. The X-ray crystal structures of compounds 5, and 7 have been determined to corroborate, both the validity of the monitored substitution processes, and the geometrical arrangement of the ligands around the Pt(IV) centre in the final complexes. Although in all cases the reaction studied takes place through the formation of a pentacoordinated intermediate and ulterior entry of the incoming ligand, the relative values of the rate constants involved in the process vary dramatically. Changes in equilibrium constants, discrimination ratio of the pentacoordinated intermediate, and dissociation rate constants can be easily associated with the relative steric and electronic characteristics of the leaving/entering ligands and solvent polarity.

2. Experimental

2.1. Instruments

¹H NMR spectra were recorded with a Varian XL-200 and Bruker 250 DMX spectrometers. Chemical shifts (in ppm) were measured relative to SiMe₄, the solvent used was acetone(*d*₆) or chloroform(*d*₁). All

spectra were obtained in the Unitat de RMN d'Alt Camp de la Universitat de Barcelona.

2.2. Products

All the methylamine ligands used in this study were obtained from distillation over NaOH from the aqueous commercially available products, pyridine and propylamine were used as purchased; solvents were distilled and keep under N₂. Complexes 1 and 2 have been prepared according to the established literature procedures [10,11]. For the preparation of the amine substituted derivatives the standard published procedure [18,19] has been also applied; characterization of the complexes has been achieved via ¹H NMR spectra (Table S1, supplementary material). Solid samples of complexes 4, 5, 6, 7, 8, and 9 have been prepared by reaction of the stoichiometric amounts of 1 with the corresponding amine in acetone or toluene solution, after 1 day, the solutions were taken to dryness and the remaining solid dissolved in the minimum amount of acetone for recrystallization. For complex 3, the solvolysis in DMSO of complex 1, followed by vacuum distillation at 60 °C, produced a solid that, after workup, could not be dissolved neither in acetone, nor in chloroform; its suspension in acetone or chloroform-containing SMe₂ or PPh₃ produced the clean spectra of compounds 1, 9. By similitude with previous studies, and the poor ligand characteristics of DMSO on Pt(IV) centres [12,20,21], the solid was assumed to the dinuclear chloride-bridged complex [{Pt(Me)₂(CCl₃CHNCH₂Ph)(μ-Cl)₂}], its solution in DMSO-containing acetone or chloroform produced solution of the desired compound 3, the value of 18 Hz for the Pt–H(SOMe₂) coupling constant indicates the S bonded nature of the ligand.

Yields were always in the 60–80% margin (*Anal. Calc.* for: 4 $\frac{1}{2}$ CH₃COCH₃, C, 34.04; H, 3.40; N, 4.29%; Found: C, 33.6; H, 3.8; N, 4.8%. *Calc.* for: 5, C, 35.0; H, 3.50; N, 4.30%; Found: C, 35.2; H, 3.7; N, 4.2%. *Calc.* for: 6, C, 33.90; H, 3.32; N, 4.39%; Found: C, 33.9; H, 5.7; N, 4.2%. *Calc.* for: 7, 0.18C₆Cl₆, C, 34.3; H, 3.30; N, 3.98%. Found: C, 34.7%; H, 3.7; N, 3.5%. *Calc.* for: 8 CH₃COCH₃, C, 39.5; H, 3.45; N, 3.84%. Found: C, 39.3; H, 3.4; N, 3.9%. *Calc.* for: 9, C, 47.77; H, 3.42; N, 1.64%. Found: C, 47.6; H, 3.4; N, 1.7%).

2.3. Crystallography

Good quality X-ray crystals from compounds 5 and 7 were obtained by cooling concentrated acetone solutions of the complexes in a refrigerator for extended periods. Selected prismatic crystals were mounted on a MAR345 diffractometer with a image plate detector and using graphite monochromated Mo Kα radiation (λ 0.71073 Å) in the ω–2θ scan mode. Unit-cell parameters were

determined from automatic centering of 9822 (5) or 25 (7) reflections ($3 < \theta < 31^\circ$) and refined by least-squares method. Lorentz-polarization and absorption corrections were made. The structure was solved by direct methods, using the SHELXS computer program [22] and refined by full-matrix least-squares method with the SHELX97 computer program. The function minimized was $\sum w||F_o|^2 - |F_c|^2|^2$ where $w = [\sigma^2(I) + (0.0385P)^2 + 11.943P]^{-1}$, and $P = (|F_o|^2 + 2|F_c|^2)/3$, f , f' and f'' were taken from International Tables of X-Ray Crystallography [23]. H atoms were computed and refined, using a riding model, with an overall isotropic temperature factor equal to 1.2 time the equivalent temperature factor of the atom which are linked. Tables S2–S7 collect relevant crystallographic data.

2.4. Kinetics

For the substitution processes, the reactions were followed by UV–Vis spectroscopy in the 500–330 nm

range where none of the solvents absorb. Runs with $t_{1/2} > 170$ s were recorded on an HP8452A instrument equipped with a thermostated multicell transport; runs within the 7–170 s margin were recorded on a HP8452A or a J&M TIDAS instrument and using a High-Tech SFA-11 Rapid Kinetics Accessory; for $t_{1/2} < 7$ s an Applied-Photophysics stopped-flow instrument connected to a J&M TIDAS spectrophotometer was used. Observed rate constants were derived from absorbance versus time traces at the wavelengths where a maximum increase and/or decrease of absorbance was observed, table S8 (supplementary material) collects the obtained k_{obs} values for all the complexes studied, as a function of the starting complex, entering amine ligand, and temperature and solvent. No dependence of the observed rate constant values on the selected wavelengths was detected, as expected for reactions where a good retention of isosbestic points is observed. The general kinetic technique is that previously described [10,11,13,18,19], pseudo-first order conditions were

Table 1
Crystal data, and relevant bond angles and distances for the crystal structure of the compounds **5** and **7**

Compound	Crystal data	Bond	Length (Å)	Bonds	Angle (°)
5		Pt–C1	2.062(6)	C1–Pt–C2	83.8(3)
Space group	Monoclinic, $P2_1/c$	Pt–C2	2.059(6)	C1–Pt–C3	99.9(3)
Formula	$\text{C}_{19}\text{H}_{23}\text{Cl}_5\text{N}_2\text{Pt}$	Pt–C3	2.015(6)	C1–Pt–N1	172.2(3)
<i>a</i> (Å)	10.4530(10)	Pt–N1	2.151(5)	C1–Pt–N2	93.5(3)
<i>b</i> (Å)	16.3740(10)	Pt–N2	2.189(6)	C1–Pt–C11	87.1(2)
<i>c</i> (Å)	13.9310(10)	Pt–Cl1	2.408(2)	C2–Pt–C3	87.1(3)
β (°)	103.4710(10)			C2–Pt–N1	88.4(2)
<i>V</i> (Å ³)	2318.8			C2–Pt–N2	176.1(3)
ρ_{calc} (g cm ^{−3})	1.867			C2–Pt–Cl1	90.6(2)
fw	651.37			C3–Pt–N1	79.2(2)
<i>Z</i>	4			C3–Pt–N2	96.2(2)
Temperature (K)	293			C3–Pt–Cl1	173.3(2)
λ (Å)	0.10697			N1–Pt–N2	94.3(2)
<i>N</i>	13935			N1–Pt–Cl1	93.5(2)
<i>N</i> ₀ ($F_o > 2\sigma$)	3821			N2–Pt–Cl1	86.5(2)
$2\theta_{\text{max}}$ (°)	50				
$R(F_o)$, $wR_2(F_o^2)$	0.0398, 0.0896				
7 $\frac{1}{2}\text{C}_6\text{Cl}_6$		Pt–C1	2.063(11)	C1–Pt–C2	85.5(6)
Space group	Monoclinic, $C2/c$	Pt–C2	2.054(11)	C1–Pt–C3	85.6(4)
Formula	$\text{C}_{22}\text{H}_{24}\text{Cl}_8\text{N}_2\text{Pt}$	Pt–C3	2.037(9)	C1–Pt–N1	89.3(4)
<i>a</i> (Å)	22.7180(10)	Pt–N1	2.146(7)	C1–Pt–N2	178.7(4)
<i>b</i> (Å)	13.5170(10)	Pt–N2	2.308(9)	C1–Pt–Cl1	90.2(3)
<i>c</i> (Å)	18.3240(10)	Pt–Cl1	2.394(3)	C2–Pt–C3	100.1(5)
β (°)	105.48			C2–Pt–N1	174.8(5)
<i>V</i> (Å ³)	5422.8(6)			C2–Pt–N2	93.3(5)
ρ_{calc} (g cm ^{−3})	1.948			C2–Pt–Cl1	87.0(4)
fw	95.127			C3–Pt–N1	80.1(4)
<i>Z</i>	8			C3–Pt–N2	95.3(3)
Temperature (K)	293			C3–Pt–Cl1	171.4(3)
λ (Å)	0.10697			N1–Pt–N2	91.9(3)
<i>N</i>	13261			N1–Pt–Cl1	92.4(2)
<i>N</i> ₀ ($F_o > 2\sigma$)	6259			N2–Pt–Cl1	89.1(2)
$2\theta_{\text{max}}$ (°)	50				
$R(F_o)$, $wR_2(F_o^2)$	0.0457, 0.1252				

maintained whenever possible, and the platinum concentration was kept at 2.5×10^{-4} M to avoid undesired decomposition reactions. No substitution reactions involving NH_2Me in acetone solution could be carried out given the undesired condensation reaction of the amine with the acetone which produced a dramatic effective decrease on the amine concentration.

3. Results

Complexes **1** and **2** have been prepared according to the literature [10,11,18,19]. Reaction of the dimethylsulfide derivatives with the corresponding ligands in acetone solution, produced the expected **6**, **7**, **8** and **9** complexes. For compounds **4** and **5** toluene solutions were used instead, due to the condensation reaction of the monoalkylamines with acetone occurring under these conditions, while for compound **3** solvolysis in DMSO of complex **1** was the method used. The complexes that have been characterized by their elemental analysis and NMR spectra (Table S1); the X-ray crystal structure determination of compounds **5** and **7** has been carried out (Table 1, Fig. 1).

The structures (Tables S2–S7, supplementary material) indicate that the products have the same geometrical arrangement than that found for most of these complexes, as expected [10–12,18,19]. In the case of **7** the crystals contain $\frac{1}{2}$ of a C_6Cl_6 molecule, per molecule of complex, which helps crystallization due to stacking of the phenyl rings. In fact the starting $\text{C}_6\text{Cl}_6\text{CHNCH}_2\text{C}_6\text{H}_5$ imine [18] had only a 5–10% of excess C_6Cl_6 , concentration on the final obtained solid is dramatically increased to 18% (see Section 2) and to the above-mentioned 50% for the X-ray quality crystals; no good crystals could be obtained with an analytically pure sample of the imine starting material. No special features are found in the structure, as a whole it seems to be less constrained in angles and distances than the previously known structures of similar complexes. The Pt–Cl bonds are longer, as expected, given the coordination of a better donor (N versus S) that produces a less acidic Pt(IV) centre. Nevertheless, it is interesting to see that, even with a small ligand such as NH_2Pr , the structure of compound **5** keeps having the *trans*^{arom}C–Cl structure found for much more crowded systems. Anyway, the relative position of the substituents on the octahedral $\text{Me–Cl–N}^{\text{amine}}$ face is revealing, while for the **7** complex the $\text{Me–Cl–N}^{\text{amine}}$ face has the same Λ -like arrangement found for similar SMe_2 and PPh_3 systems [10,11,18,19], for the **5** compound the arrangement is Δ -like, as that found for the SBzl_2 complex, **2** [11]. Furthermore, the position of the benzyl dangling arm of the imine ‘faces’ both the NH_2Pr and the SBzl_2 ligands, in their respective complexes, which seems to be

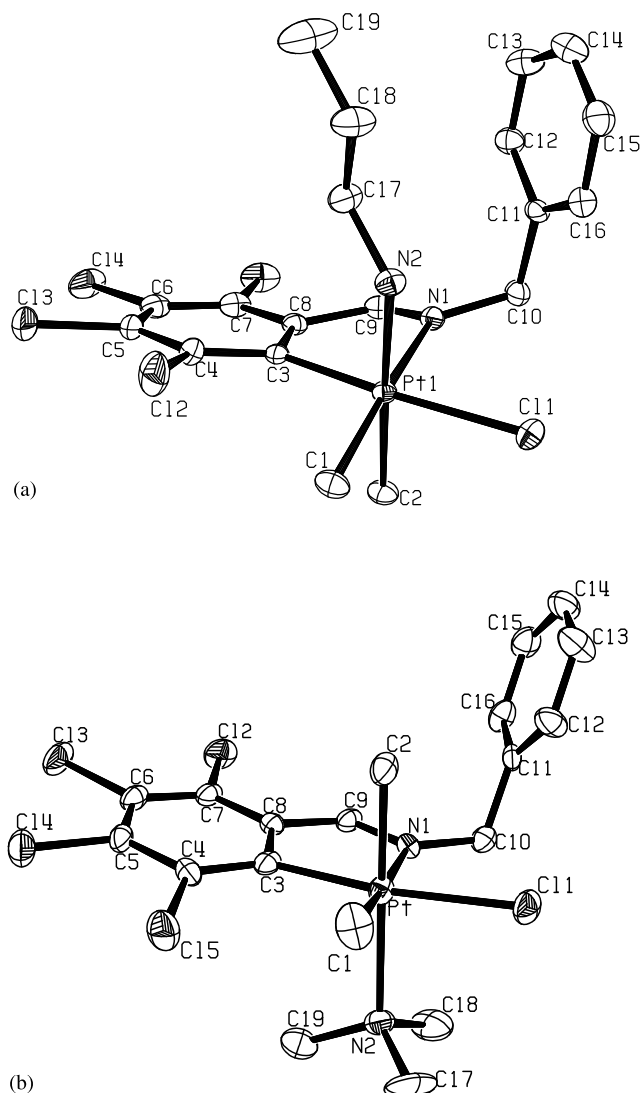


Fig. 1. View of the structures of complexes **5** (a) and **7**(b). Ellipsoids indicate 20% probability.

the less favoured available arrangement. Some sort of interaction should be established in solution that produces this form, as already kinetically detected for the SBzl_2 by phosphine substitution reactions [11,14].

^1H NMR monitoring of the substitution processes on the complexes under kinetic conditions indicated in all cases that the process is clean. Table 2 collects all the equilibrium constants derived from ^1H NMR experiments for the reactions studied kinetically; it is clear that the effect of size and donor capabilities of the leaving/entering ligands plays a crucial role for the values obtained.

The substitution reactions studied have been monitored via electronic spectroscopy in the full 500–330 nm wavelength range. The presence of only one clean process is confirmed by the retention of isosbestic points in the UV–Vis spectra over time. In some cases, and under the desired pseudo-first order conditions of the

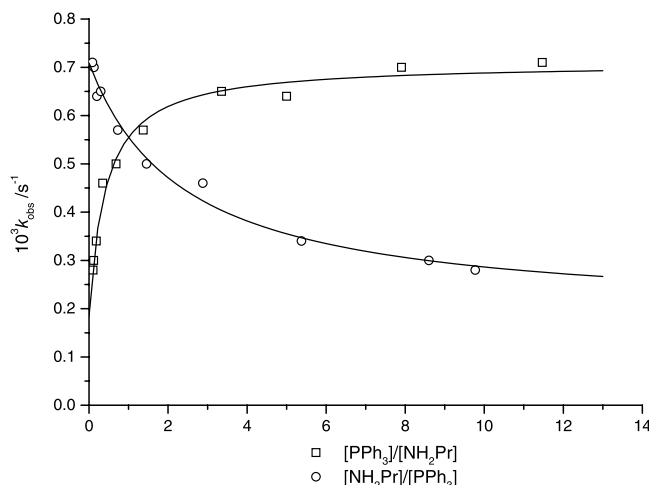


Fig. 2. Plots of the dependence of the observed rate constants on the concentration ratio of entering/leaving (○) and leaving/entering (□) ligand concentrations for the reaction of **5** with PPh₃ in toluene solution at 35 °C.

concentration of the leaving ligand, no reaction was detected, as expected from the small values of the equilibrium constants measured. In these cases the reactions were studied only in the presence of entering ligand, as the absorbance versus time traces showed a good first order behaviour [10–12]. Nevertheless, for most of the reactions studied a retardation effect on the rate constant is detected in the presence of leaving ligand in the reaction mixture; in all these cases, a concomitant direct dependence on the concentration of entering ligand is observed, Fig. 2 shows the concentration effects described.

Even so, for some of the substitution reactions studied, where an equilibrium is established, the observed reaction rate constant is found independent on both entering and leaving ligand concentrations. Fig. 3

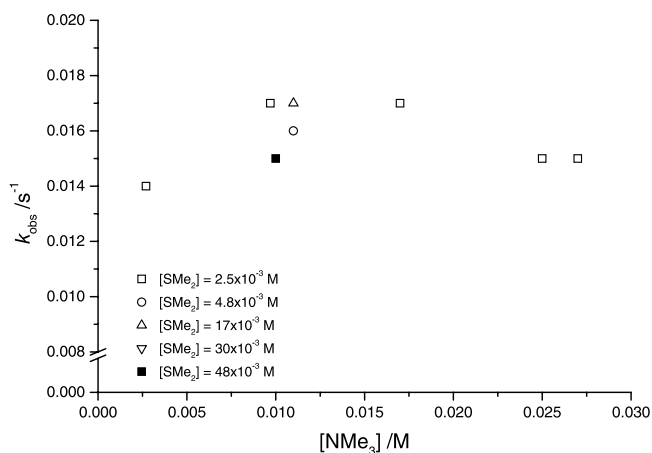
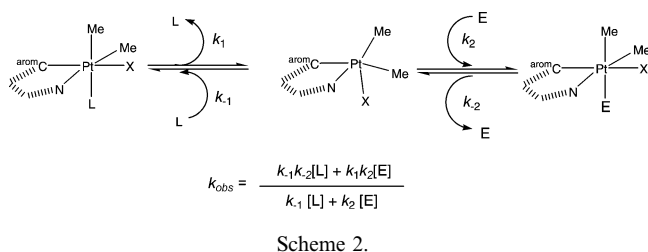


Fig. 3. Plots of the dependence of the observed rate constants on the concentration of entering and leaving ligand concentrations for the reaction of **1** with NMe₃ in acetone solution at 15 °C.

reflects the behaviour observed for the substitution processes indicated.

In view of this dependence, and our previously published work [10–13], the reaction mechanism and rate law depicted in Scheme 2 and Eq. 2 were used to fit the data for the systems indicated.



$$\begin{aligned}
 (2a) \quad k_{\text{obs}} &= \frac{k_2(k_1/k_2) + k_1([E]/[L])}{(k_1/k_2) + ([E]/[L])} \quad \left\{ \begin{array}{l} \text{large } [E] \rightarrow k_1 \\ \text{large } [L] \rightarrow k_2 \end{array} \right. \\
 k_{\text{obs}} &= \frac{k_2(k_1/k_2)([L]/[E]) + k_1}{(k_1/k_2)([L]/[E]) + 1} \\
 k_{\text{obs}} &= \text{constant} \\
 (2b) \quad k_1 &= k_2 \quad \text{then } k_{\text{obs}} = k_1 \\
 (2c) \quad k_1 &\ll k_2 \quad \text{or } k_1 k_2 \ll k_1 k_2 \quad \text{then } k_{\text{obs}} = k_1
 \end{aligned}
 \tag{2}$$

For the substitution reactions showing the saturation behaviour indicated in Fig. 2, the plots derived from the dependencies indicated in Eq. 2a were applied to calculate the values of k_1 , k_{-1}/k_2 , and k_{-2} (when measurable) from the asymptotic values and the fitted equation; the values of k_2 cannot be estimated separately, as in similar circumstances [10,24]. The substitution reactions showing a lack of any concentration dependence (Fig. 3) can only be compromised with one of the facts indicated in Eq. 2b or Eq. 2c, in both cases the value for k_{obs} becomes that for k_1 . Eq. 2c could only be applied when no equilibrium was detected (see Table 2), while Eq. 2b was applied whenever an equilibrium situation is observed with no concomitant entering or leaving ligand concentration dependence of k_{obs} . Table 3 collects all the kinetic and thermal activation parameters for the dissociation processes studied (k_1 , and ΔH_1^\ddagger and ΔS_1^\ddagger), while Table 4 collects the kinetic parameters related with the reversibility of the whole process (k_{-2}) and the pentacoordinated intermediate discrimination factor (k_{-1}/k_2). For complexes **1** and **2**, the values of k_1

determined in this study agree within the 95% margin of the predicted values derived for the SMe_2 by phosphine substitution processes previously studied, consequently their thermal activation parameters are those previously described [10,11]. Fig. 4, clearly indicates the validity of the reaction mechanism indicated in Scheme 2, the Eyring plots of k_1 and k_{-2} , for those systems where these values correspond to the same process, agree within error; the activation parameters collected in Table 3 are derived from the global fitting.

4. Discussion

The trends obtained for the equilibrium constants measured for the systems depicted in Table 2 could be explained on the basis of the varying the stereo-electronic characteristics of the entering and leaving ligands. The degree of advance of the sulfide by NMe_3 substitution on **1**, **2** and **3** observed is perfectly consistent with the difference in the size of the SMe_2 , SBzl_2 and SOMe_2 ligands, despite of the important differences in the inductive effects of the two sulfides. The greater basicity and smaller cone angle of the NH_2Me and NHMe_2 entering ligands (NH_2Me , $\text{p}K_a$ 10.6, $\theta = 106^\circ$; NHMe_2 , $\text{p}K_a$ 10.8, $\theta = 119^\circ$; NMe_3 , $\text{p}K_a$

Table 2

Values of the equilibrium constants measured for the substitution processes studied

Complex	Leaving ligand (L)	Entering ligand (E)	K_{eq}
1	SMe_2	NH_2Me	n.d.
		NH_2Pr	n.d.
		NHMe_2	n.d.
		NMe_3	0.67
2	SBzl_2	py	n.d.
		NH_2Me	n.d.
		NHMe_2	n.d.
		NMe_3	3.4
3	SOMe_2	NMe_3	n.d.
		PPh_3	n.d.
4	NH_2Me	PPh_3	3.0
5	NH_2Pr	PPh_3	2.0
6	NHMe_2	PPh_3	13
7	NMe_3	PPh_3	n.d.
8	py	py	n.d.
		PPh_3	7.7

Measured at room temperature in CDCl_3 solution; n.d., indicates that no equilibrium was detected under the kinetic conditions used in the study.

9.8, $\theta = 132^\circ$) [15–17] seems to be the dominant factor for the complete displacement of the equilibrium for the formation of the amine complexes under the conditions used. The substitution process of the amine ligands by

Table 3

Summary of kinetic and thermal activation parameters for the leaving ligand reactions studied; phosphine data from references [18,19]

Complex	Leaving ligand (L)	Entering ligand (E)	Solvent	$^{298}k_1$ (s^{-1})	ΔH_1^\ddagger (kJ mol^{-1})	ΔS_1^\ddagger (kJ mol^{-1})
1	SMe_2	Phosphines	Acetone Chloroform	0.04	91 ± 3	31 ± 10
		NH_2Me NH_2Pr NHMe_2 NMe_3	Acetone Toluene	*	*	*
		py	Acetone	0.53	57 ± 2	-62 ± 8
		Phosphines	Chloroform	*	*	*
2	SBzl_2	NHMe_2 NMe_3	Acetone	*	*	*
		Phosphines	Toluene	0.91	78 ± 2	15 ± 7
		NH_2Me NHMe_2 NMe_3	Toluene	*	*	*
		PPh_3	Acetone	19	62 ± 2	-12 ± 6
3	SOMe_2	PPh_3	Toluene	13	56 ± 2	-37 ± 6
4	NH_2Me	PPh_3	Toluene	0.00011	105 ± 1	29 ± 3
5	NH_2Pr	PPh_3	Toluene	0.00018	111 ± 3	50 ± 20
6	NHMe_2	PPh_3	Acetone	0.00018	94 ± 11	-4 ± 30
			Toluene	0.00032	107 ± 4	46 ± 13
7	$^a\text{NMe}_3$	PPh_3	Acetone	0.81	105 ± 4	84 ± 12
		py	Toluene	0.0031	91 ± 4	11 ± 14
8	py	PPh_3	Toluene	0.0031	91 ± 4	11 ± 14
9	$^b\text{PPh}_3$	py	Toluene	0.0001	112 ± 3	52 ± 11

* indicates that the values agree with the phosphine substitution processes.

^a Fitting includes k_{-2} data from SMe_2 and SBzl_2 by NMe_3 substitution, see Fig. 4^b.

Table 4

Summary of the kinetic parameters related with the reversibility of the process and the pentacoordinated intermediate discrimination factor

Complex	Leaving ligand (L)	Entering ligand (E)	Solvent	k_{-1}/k_2 ^a	$^{298}k_{-2}$ (s ⁻¹)
1	SMe ₂	Phosphines	Acetone	1.1	n.d.
			Chloroform		
		NH ₂ Me	Toluene	0.5	n.d.
		NH ₂ Pr	Toluene	0.8	n.d.
		NHMe ₂	Acetone	1.1	n.d.
			Toluene		
2	SBzl ₂	NMe ₃	Acetone	n.d.	Equals to k_1
			Toluene		
		Phosphines	Acetone	1.1	n.d.
			Chloroform		
		NHMe ₂	Acetone	2.0	n.d.
		NMe ₃	Acetone	3.2	0.062
3	SOMe ₂	NH ₂ Me	Toluene	0.4	n.d.
		NHMe ₂	Toluene	1.5	n.d.
		NMe ₃	Toluene	2.0	0.062
		PPh ₃	Acetone	1.0	n.d.
			Toluene	2.0	n.d.
4	NH ₂ Me	PPh ₃	Toluene	n.d.	Equals to k_1
5	NH ₂ Pr	PPh ₃	Toluene	0.8	0.00010
6	NHMe ₂	PPh ₃	Acetone	6.5	0.000070
		PPh ₃	Toluene	2.2	n.d.
7	NMe ₃	PPh ₃	Acetone	0.7	n.d.
		py	Toluene		
8	py	PPh ₃	Toluene	1.7	0.000080 ^b

^a Average for the conditions studied.^b From the global fitting indicated in Table 3, see Fig. S 1.

PPh₃ on complexes **4**, **5**, **6** and **7** follows the same trend found for the sulfide leaving ligands, the cone angles of the leaving ligand seem to be the dominant factor for the equilibrium displacement position, despite the variation in pK_a values. In this respect substitution by pyridine (pK_a 5.19) on complex **1** does not follow the same trend than that for the alkylamines; probably the important electronic changes introduced on the nitrogen donor are too important for the maintenance of the trend obtained with the NH₂Me, NHMe₂ and NMe₃ sequence.

The simple kinetic behaviour shown by the substitution processes studied on complexes **1** and **2** agrees well with that found for the substitution processes with phosphines [10–12]. Even the differences detected on changing the solvent, when possible (see Section 2), due to solvent-assisted interactions with the leaving SBzl₂ ligand on complex **2** substitutions are equivalent (Table 3) [11]. Only for the **1** plus NMe₃ systems the kinetic behaviour is too simple to evaluate the k_{-1}/k_2 parameter (Table 4), the data are interpreted according to Eq. 2b. Although having $k_1 = k_{-2}$ seems too much of a coincidence, it is clear that if $k_{-1} \ll k_2$ (or $k_{-1}k_{-2} \ll k_1k_2$), according to Eq. 2c, is the responsible of the observed concentration dependence, the approximation should held even more strongly for complex **2**, where k_{-1} is expected to be smaller. This is not so, and consequently it has to be $k_1 = k_{-2}$, as corroborated by Fig. 4 which shows the Eyring plot corresponding to the

dissociation of the Pt–NMe₃ bond under different premises. The same assumption applies for the **4** plus PPh₃ system given the fact that the equilibrium is not fully displaced (Figure S1). It is interesting to note that only for systems having more positively charged proton centres in the leaving ligand (SBzl₂, SOMe₂, and NHMe₂) an important difference in the thermal activation parameters of the dissociation rate constants is obtained in acetone and toluene. For the SBzl₂ and NHMe₂ complexes (**2**, **6**) the values for k_1 are smaller in acetone due to the difficulties in the dissociation, while the values of the thermal activation parameters have a tendency for a more ordered and less enthalpic demanding transition state. It seems clear that the postulated solvent-assisted interaction between the leaving ligand and the Pt skeleton for these systems is operative [11]. Surprisingly, for the DMSO complex, **3**, the opposite trend is observed, indicating that these type of interaction has to have different characteristics. The fact that the oxygen at the pyramidal SOMe₂ can cancel the charge separation of the ligand itself could prevent the above mentioned solvent-assisted electrostatic interaction with the rest of the molecule. Even so, the thermal activation parameters indicated for the reaction do not seem to agree very well with this fact, the activation entropy in toluene solution being clearly negative. Taking into account that the amount of DMSO present in the solutions is very high (see Table S8), due to the

very labile character of the ligand (see Section 2), the polarity of the solvents must be dramatically modified, specially that of toluene. In this case the trend observed in Table 3 for the substitution by PPh_3 on compound 3 agree with the results for the substitution of complexes 2 and 6, and those for other complexes [11]. If this is the case, the solvent assistance in toluene should be reinforced by the high concentration of DMSO in the solution medium, while for acetone the differences should be at a minimum. As a whole, the Pt– SOMe_2 bond dissociation occurs both in toluene and acetone solutions with a certain degree of ordering derived from the acetone and/or DMSO assistance in the interactions with the Pt complex inert skeleton. Consequently the activation enthalpies are low as expected from this ordering [11].

The trend indicated by the $^{298}k_1$ data of Table 3 is a clear indicative of the strength of the Pt–leaving ligand bond that includes both enthalpic and entropic components. That is, not only are the enthalpic demands important for the dissociation but also the degree of dissociation needed to reach the transition state. This is very well shown in the complexes with NH_2Me and NMe_3 as leaving ligands, where, despite the fact that similar enthalpic demands apply, the degree of dissociation on the amine in the transition state is larger for the more bulky NMe_3 . The trend indicates that the effective substitution strength of the Pt–L bond is $\text{PPh}_3 > \text{py} > \text{NH}_2\text{Me} > \text{NHMe}_2 > \text{NMe}_3 > \text{SMe}_2 > \text{SBzl}_2 > \text{SOMe}_2$, which is not in line with the expected for the theoretically hard Pt(IV) centre; no doubt that the presence of three Pt–C bonds in the complex produces important changes in the hardness of the centre. Nevertheless, the steric demands included in the cone angle of the

different leaving ligands are evident. Furthermore, when differences attributable to the presence of suitable proton centres that allow solvent-assisted interactions with the leaving ligand, are present, the trend in the values found for $^{298}k_1$ parallel the observed differences in the values of ΔS^\ddagger , indicating the ordering occurring on such interactions. In this respect, all the values determined for k_{-1}/k_2 for compounds 2 and 6, and collected in Table 4, indicate that the back entrance of the leaving ligand with suitable proton centres is favoured in acetone when compared with the same value in toluene, as would be expected. The opposite trend is observed for the substitutions on complex 3, nevertheless the reasons indicated above (fairly concentrated toluene solutions of DMSO being de facto more polar) point to the same type of process.

The surprising lack of an important discrimination factor found in the k_{-1}/k_2 ratio of Table 4 for this intermediate has already been detected, but the same behaviour has already been found for other processes involving isolated pentacoordinate intermediates [10–12]. It is interesting to note, though, that the trend observed for the available k_{-1}/k_2 data does not correspond to that observed for k_1 . That is, although PPh_3 is a worse leaving ligand than NHMe_2 , according to the dissociation rate constant, the proposed pentacoordinated intermediate favours the entrance of NHMe_2 in front of PPh_3 . Important solvent-assisted interactions are bound to be operating, specially in polar solutions, where the discrimination factors increase to larger values. When either solvent (or solution polarity) or leaving ligand (NMe_3) do not allow these type of interactions, these ratios approach to unity as found in most of the systems.

Finally, the existence of the k_{-2} term in Eq. 2 (Tables 2 and 4) is easily related with the sequence of substitution bond strength mentioned above. Only for systems with entering and leaving ligands close in the sequence, simultaneous observation of k_1 and k_{-2} has been possible.

Acknowledgements

We acknowledge financial support for the BQU2001-3205 project from the Ministerio de Ciencia y Tecnología.

References

- [1] M.L. Tobe, J. Burgess, *Inorganic Reaction Mechanisms*, Addison-Wesley, Reading, MA, 1999.
- [2] M.V. Twigg, *Mechanisms of Inorganic and Organometallic Reactions*, Plenum, New York, 1991.
- [3] D.D. Wick, K.I. Goldberg, *J. Am. Chem. Soc.* 119 (1997) 10235.

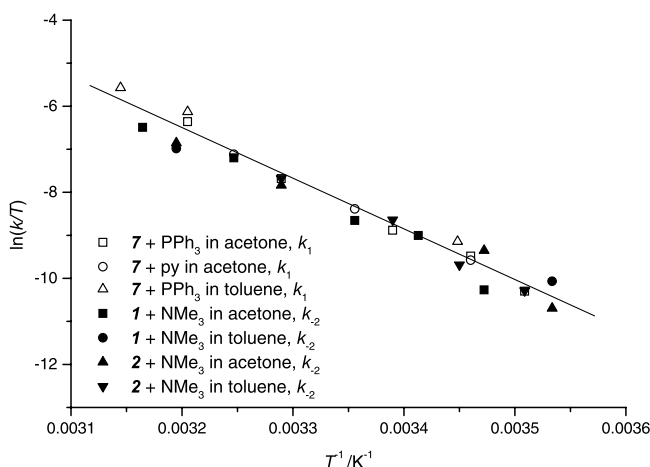


Fig. 4. Combined Eyring plot for the substitution reactions of NMe_3 by PPh_3 and py on the studied complex skeleton. Open symbols indicates k_1 for the process occurring on 7; solid symbols refer to k_{-2} for the inverse process taking place on 1 and 2.

- [4] C.R. Baar, G.S. Hill, J.J. Vittal, R.J. Puddephatt, *Organometallics* 17 (1998) 32.
- [5] J.R. Alger, J.H. Prestegord, *J. Magn. Resonance* 27 (1977) 137.
- [6] T. Shi, J. Berglund, L.I. Elding, *Inorg. Chem.* 35 (1996) 3498.
- [7] S. Choi, S. Mahalingaiah, S. Delaney, N.R. Neale, S. Massod, *Inorg. Chem.* 38 (1999) 1800.
- [8] M.D. Hall, T.W. Hambley, *Coordin. Chem. Rev.* 232 (2002) 49.
- [9] A. Peloso, *Coordin. Chem. Rev.* 10 (1973) 123.
- [10] P.V. Bernhardt, C. Gallego, M. Martinez, *Organometallics* 19 (2000) 4862.
- [11] P.V. Bernhardt, C. Gallego, M. Martinez, T. Patella, *Inorg. Chem.* 41 (2002) 1747.
- [12] M. Font-Bardía, C. Gallego, G. González, M. Martinez, A.E. Merbach, X. Solans, *J. Chem. Soc., Dalton Trans.*, in press.
- [13] M. Font-Bardía, C. Gallego, M. Martinez, X. Solans, *Organometallics* 21 (2002) 3305.
- [14] H. Kumita, T. Kato, K. Jitsukawa, H. Einaga, H. Masuda, *Inorg. Chem.* 40 (2001) 3936.
- [15] A.L. Seligson, W.C. Trogler, *J. Am. Chem. Soc.* 113 (1991) 2520.
- [16] T.L. Brown, K.J. Lee, *Coord. Chem. Rev.* 128 (1993) 89.
- [17] R.M. Smith, A.E. Martell, *Critical Stability Constants*, Plenum, New York, 1989.
- [18] M. Crespo, M. Martínez, E. de Pablo, *J. Chem. Soc., Dalton Trans.* (1997) 1231.
- [19] M. Crespo, M. Martínez, J. Sales, *Organometallics* 12 (1993) 4297.
- [20] R. Romeo, M.R. Plutino, L.M. Scolaro, S. Stoccoro, G. Minghetti, *Inorg. Chem.* 39 (2000) 4749.
- [21] R. Romeo, *Comments Inorg. Chem.* 11 (1990) 21.
- [22] G.M. Sheldrick, *SHELXL97*, Program for Crystal Structure Determination, University of Göttingen, Göttingen, Germany, 1997.
- [23] *International Tables of X-Ray Crystallography*, Kynoch Press, Birmingham, 1974.
- [24] J.H. Espenson, *Chemical Kinetics and Reaction Mechanisms*, McGraw-Hill, New York, 1995.